California Energy Commission
Public Interest Energy Research Program

LBNL No. 50678
(HPCBS No E5P23T3d)

HPCBS

High Performance Commercial Building Systems

Field Testing of Component-Level Model-Based Fault Detection Metho

Element 5
Project 2.3
Task 2.3.3

Peng Xu and Philip Haves
Ernest Orlando Lawrence Berkeley National Labora

pier
PUBLIC INTEREST ENERGY RESEARCH
"Research Powers the Future"

LBNL-50678
CD-452

Presented at the ACEEE 2002 Summer Study on Energy Efficiency in Buildings, August 18-23, 2002, Asilomar Conference Center, Pacific Grove, California, and published in the proceedings.

Field Testing of Component-Level Model-Based Fault Detection Methods for Mixing Boxes and VAV Fan Systems

Peng Xu and Philip Haves

Building Technologies Department
Environmental Energy Technologies Division
Ernest Orlando Lawrence Berkeley National Laboratory
University of California
1 Cyclotron Road
Berkeley, California 94720-8134 USA

May 2002

This work was supported by the California Energy Commission Public Interest Energy Research Program and by the Assistant Secretary for Energy Efficiency and Renewable Energy, Office of Building Technology, State and Community Programs, Office of Building Research and Standards of the U.S. Department of Energy under Contract No. DE-AC03-76SF00098.

Field Testing of Component-Level Model-Based Fault Detection Methods for Mixing Boxes and VAV Fan Systems

Peng Xu and Philip Haves
Building Technologies Department, Environmental Energy Technologies Division
Lawrence Berkeley National Laboratory

Abstract

An automated fault detection and diagnosis tool for HVAC systems is being developed, based on an integrated, life-cycle, approach to commissioning and performance monitoring. The tool uses component-level HVAC equipment models implemented in the SPARK equation-based simulation environment. The models are configured using design information and component manufacturers' data and then fine-tuned to match the actual performance of the equipment by using data measured during functional tests of the sort using in commissioning. This paper presents the results of field tests of mixing box and VAV fan system models in an experimental facility and a commercial office building. The models were found to be capable of representing the performance of correctly operating mixing box and VAV fan systems and detecting several types of incorrect operation.

Introduction

There is a growing consensus that most buildings do not perform as well as intended and that faults in HVAC systems are widespread in commercial buildings. There is a lack of skilled people to commission buildings and commissioning is widely seen as too expensive and/or unnecessary. There is also a lack of skilled people, and procedures, to ensure that buildings continue to operate efficiently after commissioning. One approach to these problems is to wholly or partly automate both commissioning and performance monitoring, using computer-based methods of fault detection and diagnosis (FDD). Component-level FDD, which is the subject of the work presented here, uses a bottom up methodology to detect individual faults by analyzing the performance of each component in the HVAC system (Hyvarinen 1997, LBNL 1999, Haves & Khalsa 2000).

Model-based approaches to fault detection for different HVAC system or sub system have been proposed by various researchers. Benouarets et al. (1994) describe two model-based schemes for detecting and diagnosing faults in air-conditioning systems. They examined their ability to detect water-side fouling and valve leakage in the cooling coil subsystem of an air handling unit. McIntosh et al. (2000) developed a mechanical model for fault detection and diagnosis in chillers. The model was calibrated using data from an operating system and was used in identifying operating faults. Ahn et al. (2001) present a model-based method for the detection and diagnosis of faults in the cooling tower circuit of a central chilled water facility. Faults are detected from deviations in the values of the characteristic quantities from the corresponding values for fault-free operation. The patterns of the deviations are different for each fault, allowing rules to be developed that can be used to diagnose of the source of the fault.

For commissioning, a baseline model of correct operations is normally first configured and adjusted using design information and manufacturers' data. Next, the behavior of the equipment measured during functional testing is compared to the predictions of the model; significant differences indicate the presence of one or more faults. Once the faults have been fixed, the model is fined-tuned to match the actual performance observed during the functional tests performed to confirm correct operation. The model is then used as part of a diagnostic tool to monitor performance monitoring diagnostic tool during routine operation. In each case, the reference model is used to predict the performance that would be expected in the absence of faults. A comparator is used to determine the significance of any differences between the predicted and measured performance and hence the level of confidence that a fault has been detected.

The performance of a model-based fault detection tool is critically dependent on the ability of the model to represent the performance of correctly operating equipment in the field. The paper presents the results of tests to assess how well simple models can represent the performance of HVAC secondary systems (air handling units and distribution systems). The tests were performed at the Iowa Energy Center's Energy Resources Station and in a commercial office building in San Francisco, California.

Component Models

The simulation program SPARK - Simulation Problem Analysis and Research Kernel (SPARK 2002) was used to develop and implement the component models. SPARK is an object-oriented software system that can be used to simulate physical systems that can be modeled using sets of differential and algebraic equations. One advantage of SPARK is that a solution procedure for the model equations is generated automatically, leaving the developer free to concentrate on specifying the equations that define the behavior of the component.

The models addressed in this paper are listed in **Table 1**, along with the measurements that are assumed to be available as inputs to the model. A brief description of each model is presented below; a more detailed description is presented in Xu and Haves (2001). The use of the models for functional testing and for performance monitoring is explained and illustrated in subsequent sections.

Table 1. Inputs And Outputs Of Models

	Inputs	Output
Mixing box	• control signal to damper actuators • outside air temperature • return air temperature • outside air humidity • return air humidity	• mixed air temperature • mixed air humidity N.B. Since mixed air temperature is often not measured and mixing is often incomplete anyway, supply air temperature (corrected for temperature rise across the supply fan) is often used as a proxy for mixed air temperature when the coils are inactive.
VAV fan system	• fan speed (assumes variable speed drive) • volumetric air flow rate	• supply fan: supply duct static pressure • return fan: room pressure (may be assumed to be ~0.1inH_2O if not measured) • fan pressure rise • fan power

One issue in modeling for fault detection is that some degree of imperfect operation may be tolerated in practice (e.g., leakage of valves or dampers) and so must be included in models that ostensibly represent correct operation.

Mixing Box

Prediction of the mixed air temperature and humidity in an air handling unit involves estimating the outside and return air fractions and then performing heat and moisture balances on the mixed air stream. Prediction of the air-flow fractions from the control signals to the actuators that position the dampers is impractical because (i) the return air and mixing plenum pressures change with fan speed and (ii) it is difficult to estimate air-flow resistances in mixing boxes. This said, the behavior in the middle of the operating range is relatively unimportant compared to the behavior at each end of the operating range. An empirical approach to modeling the airflow fractions has therefore been adopted.

The mixing box model is shown in **Figure 1**. At the commissioning stage, when only design information is available, the range of acceptable behavior is modeled. A 3:1 gain variation is used by default; when the damper position is 50%, the permitted upper limit of the outside air fraction is 75% and the lower limit is 25%. The maximum acceptable deviations from 0 and 100% outside air fraction at each end of the operating range, which are determined by the leakage in the dampers, should be specified by the designer based on manufacturer's data. Note

that leakage can arise from imperfections in the dampers themselves, their incorrect installation in the duct or from a mismatch between the ranges of operation of the damper and its actuator. Once the mixing box has been commissioned, the results of the functional test can be used to fit a third order polynomial to the measured variation of the outside air fraction with the control signal to the damper actuator.

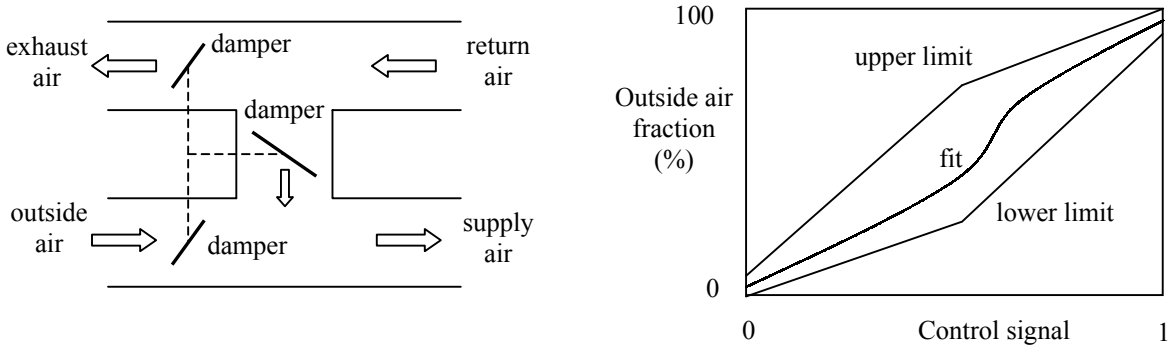

Figure 1. The mixing box model.

VAV Fan System

The model treats VAV systems that have fans with variable speed drives. The supply and return sections are considered separately, as shown in **Figure 2.**

Fan performance is modeled by using the fan similarity laws to normalize the volumetric flow rate, V, pressure rise, Δp_{fan}, and power, P, in terms of the rotation speed, n_{fan}. Over the limited range of normalized flow used in normal operation, the fan head curve can be approximated using a constant term and a squared term. The constant term is the pressure rise extrapolated to zero flow rate, which is proportional to the square of the rotation speed,

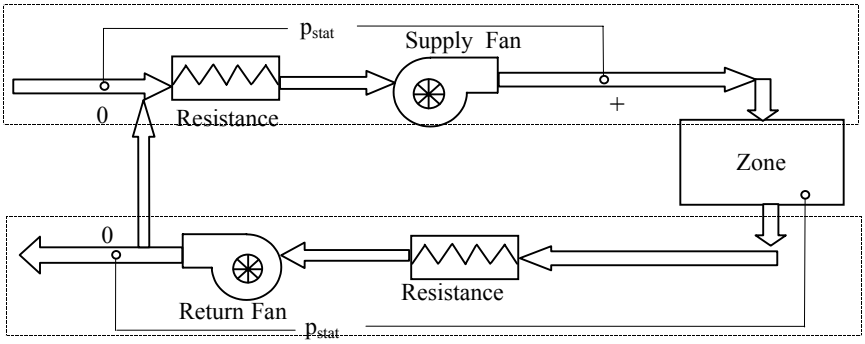

Figure 2. Diagram of VAV fan system showing sections covered by the model.

and the squared term corresponds to the pressure drop inside the fan. The model is written in terms of total pressure (i.e., static pressure plus velocity pressure) since energy losses are directly related to changes in total pressure. The pressure rise across the fan is then:

$$\Delta p_{fan} = k_{fan} n_{fan}^2 - C_{fan} V^2 \qquad (1)$$

where k_{fan} and C_{fan} are empirical constants that will be determined initially from manufacturer's head curve data or from field measurements of flow rate, pressure rise and rotation speed.

The pressure rise across the fan is balanced by the system pressure drop, which consists of the pressure drop in the other air handling unit (AHU) components and in the distribution system components. The pressure drop, Δp_{res}, can also be represented by a constant term and a squared term. For the supply fan subsystem, the constant term is the static pressure in the supply duct, p_{stat}. The squared term represents the pressure drop through the AHU and

distribution system components, $C_{res}V^2$, and the velocity pressure at the static pressure sensor ($\rho V^2/2A^2$, where ρ is the density and A is the cross sectional area of the duct), both of which are proportional to the square of the air mass flow rate.

$$\Delta pres = pstat + (Cres + \rho/2A2)V2 \quad (2)$$

For the return fan subsystem, p_{stat} is the measured or assumed pressure in the occupied space and appears as a negative term in Equation 3, since a positive pressure in the space reduces the fan pressure rise required. The correction for the velocity pressure in the room is very small and can be ignored.

$$\Delta pres = -pstat + CresV2 \quad (3)$$

Combining the equations for the pressure rise across the fan and the system pressure drop yields:

$$pstat = kfannfan2 – (Cfan + Cres + \rho/2A2)V2 \quad (4)$$

which is used to predict the measured static pressure in the duct (or the pressure in the space) from the fan speed and the air flow rate. If the airflow rate is not measured but there are measurements of fan power and fan pressure rise, the airflow rate can be estimated directly if the combined efficiency of the motor and fan, η, is known from catalog data or one time measurement:

$$V = \eta P / \Delta pfan \quad (5)$$

If the fan power is measured but the fan pressure rise is not, the airflow rate can be estimated by solving:

$$V = \eta P / (kfannfan2 - CfanV2) \quad (6)$$

Note that it is not possible to determine the flow rate and the efficiency independently. The flow rate must be measured in order to determine the efficiency. The efficiency can be assumed to be constant over the range of operation or it can be approximated by a quadratic relationship in the normalized flow rate, V/n, about the maximum value, η_{max}:

$$\eta = \eta max – E(V/n – Vmax/n)2 \quad (7)$$

Finally, when assessing the thermal performance of the mixing box and coils, it is useful to be able to use the measurement of supply air temperature as a proxy for the mixed air temperature or the off-coil air temperature. In a draw-through system, this requires correcting for the temperature rise, ΔT, across the fan, which can be estimated from the pressure rise and the efficiency:

$$\Delta T = \Delta P/\eta\, \rho cp \quad (8)$$

A summary of the data requirements for VAV fan system and the data source is given in **Table 2**.

Table 2. Requirements For VAV Fan System Data

Parameter	Requirement	Source
Fan speed	Required	Measured
Volumetric air flow rate	Required	Measured or calculated using eq.5 or eq.6
Supply duct static pressure	Required	Measured
Room pressure	Required	Measured
Fan pressure rise	Required if air flow rate unknown or can not calculated from fan power	
Fan power	Required	Measured
Fan/motor efficiency	Required if airflow rate is unknown or fan pressure rise is unknown	Catalog data or calculated using Eq.7 based on one time measurement
Fan temperature rise	required for mixing box calibration	Measured or calculated using Eq. 8

Modeling Using Measured Data From An Experimental Facility

The models described above were tested using data that are expected to be representative of the measurements that would be obtained from well controlled functional testing. The measurements were made by others under well-controlled conditions using the HVAC systems at the Iowa Energy Center's Energy Resource Station (ERS). The ERS is configured like a real building but is operated as an experimental facility. One advantage of the ERS is that the sensors are regularly calibrated, so that sensor error is unlikely to confound the experimental results. The HVAC system at the ERS consists of three different air-handling units that are controlled by commercial energy monitoring and control systems. The data used here are from Air Handling Unit A and are the results of two sets of step tests on the mixing box and the fans. All the step tests were open loop tests that were conducted by overriding the feedback controller and adjusting the output signal from minimum to maximum, and from maximum to minimum, in a predetermined series of small steps. Relatively large numbers of steps were employed in order to determine which particular steps provide the most useful information. It is anticipated that the tests used in practice will use fewer steps.

The purpose of the tests reported here was twofold:

1. To verify the forms of the relationships used in the models by verifying that the models can be made to fit the data by choosing suitable values for the model parameters.
2. To verify that models with parameter values derived from design information and manufacturers' data can be used to predict the performance of correctly operating systems.

Model Calibration Procedures

Mixing Box. The parameters of the mixing box model are the fractional leakage flows at each end of the operational range and the coefficients of the polynomial relationship between outside air fraction and damper position. Since the leakage parameters are considered to be the most important and they can be determined directly from the measurements at each end of the range of operation, they are determined first. The remaining coefficients in the third order polynomial are then determined by applying the method of least squares to the rest of the measurements. If there is a significant amount of hysteresis, separate fits are performed for opening and closing.

Fan System. Because measurements of fan pressure rise and fan power are available in addition to measurements of airflow rate and static pressure, the calibration of the fan system model was divided into three steps. First, the values of the two parameters (k_{fan}, C_{fan}) of the simplified fan model (Equation 1) were determined from the measurements of fan pressure rise, fan speed and airflow rate. Next, the value of the system pressure loss coefficient, $C_{res,}$ was determined by minimizing the error in the pressure predicted using Equation 4. Lastly, the parameters of the motor and fan efficiency model (Equation 7) were determined from the measurements of fan power, speed, pressure rise, and airflow rate. In each case, the parameters were determined by the method of least squares.

Results

The results for the mixing box test are shown in **Figure 3**. The measurements of the outside, return and mixed air temperatures and the demanded position of the damper actuators are shown in **Figure 3A**. Since there is relatively poor mixing in most mixing boxes, the supply air temperature, corrected for the rise across the supply fan using Equation 8, is used as a proxy for the mixed air temperature. The maximum mixed air temperature is very close to the return air temperature and the minimum mixed air temperature is very close to the outside air temperature, indicating that leakage is small. **Figure 3B** is a comparison of the measured mixed air temperature and the mixed air temperatures corresponding to the 3:1 gain range described above and shown in **Figure 1**. The measured values lie between the permitted upper and lower limits, except when the demanded position of the damper is 10%,

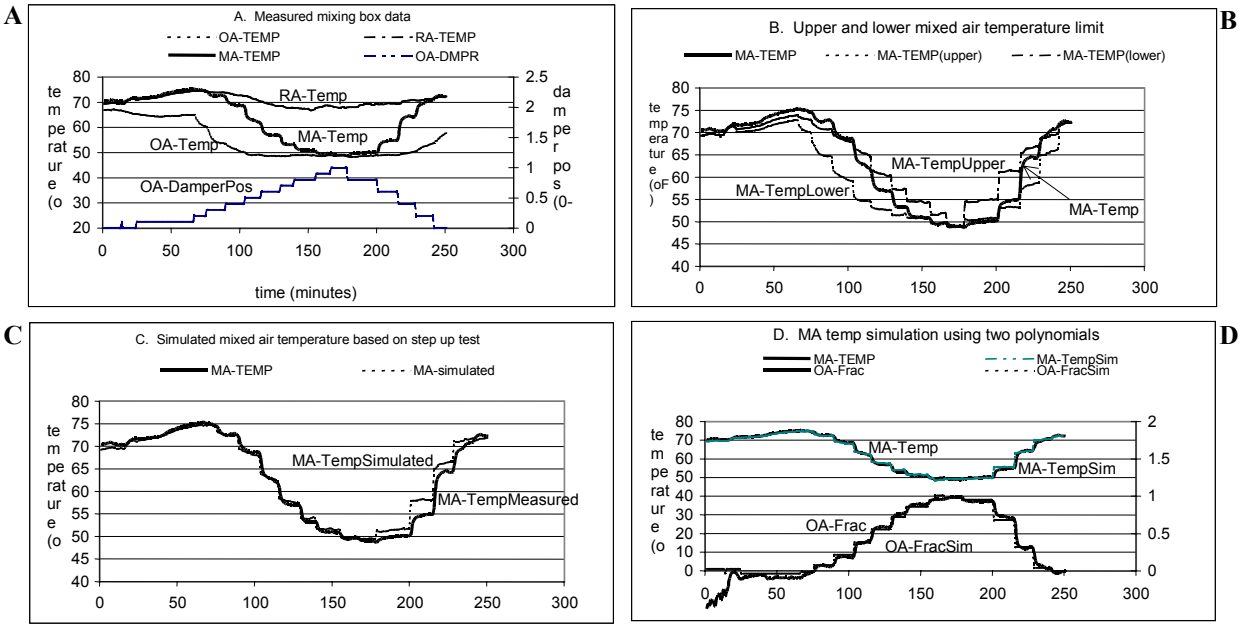

Figure 3. Mixing box calibration (experimental data).

when the damper fails to open significantly, in part because of hysteresis. **Figure 3C** shows the simulated mixed air temperature, based on the polynomial fit to the data obtained when the outside damper was being stepped open. The deviations between the predictions and the measurements obtained when the dampers were stepped in the opposite direction indicate the presence of hysteresis. **Figure 3D** shows the simulated mixed air temperature and outside air fraction using two polynomials for the damper operation, one for opening and one for closing.

Figure 4 shows examples of fault detection using measurements of mixing box performance made when the return air damper had been fixed in the closed position. The outside and exhaust air dampers were closed in 10% steps and then opened in 20% steps, as shown in **Figure 4A**. In automated commissioning, such faults can be detected during the functional testing phase if the measured mixed air temperature lies outside the permitted range, as can be seen in **Figure 4B**. During routine operation, the fault can be detected by comparing the measured and simulated mixed air temperatures (**Figure 4C**) or the measured and simulated outside air fractions (**Figure 4D**).

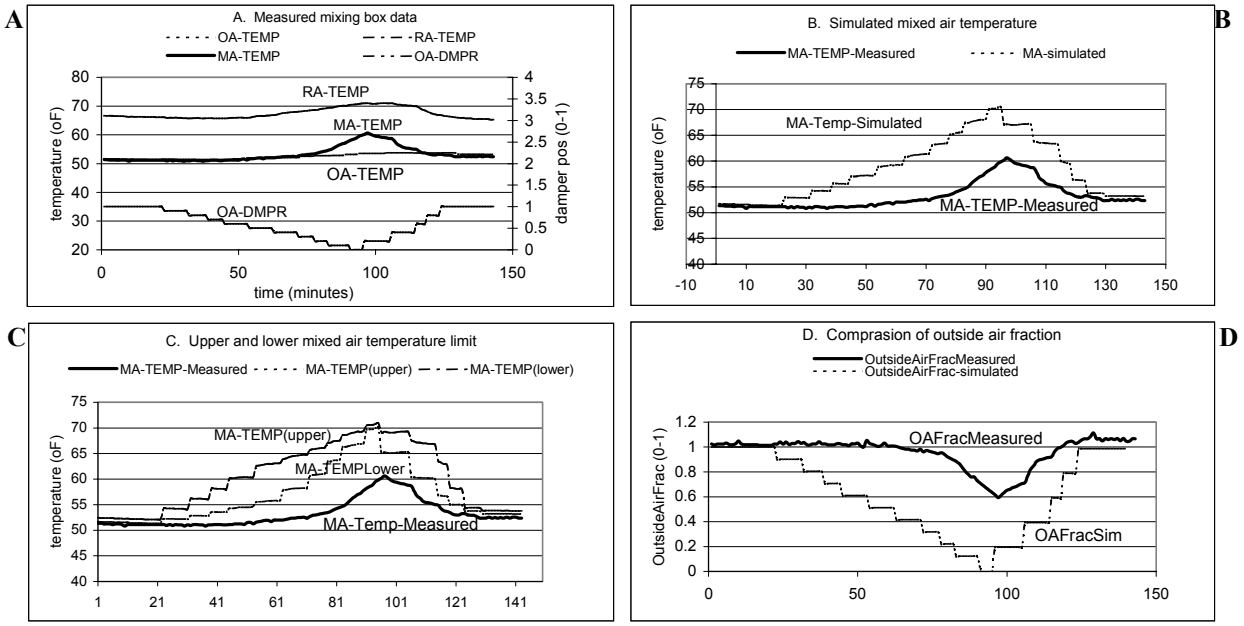

Figure 4. Mixing box fault detection (experimental data).

Figure 5 shows the results for the supply fan system at the Energy Resource Station. The parameters of the model were first estimated from design information. The fan parameters were estimated from the manufacturer's head and efficiency curves. The system resistance was estimated from the rated pressure drops at design airflow of the major system components: the heating and cooling coils used to precondition the outside air, the filter and the main heating and cooling coils. **Figures 5B** and **5C** show the predicted and measured static pressure and fan pressure rise. Both graphs show significant differences at intermediate fan speeds. The presence of significant differences in **Figure 5C** indicates a fault in the fan. Examination of **Figure 5A** shows that there was a significant flow rate (~14% of full speed) when the demanded speed was zero. The problem was subsequently traced to a defect in the variable speed drive, confirming that a real fault had been detected. When an approximate correction was applied to

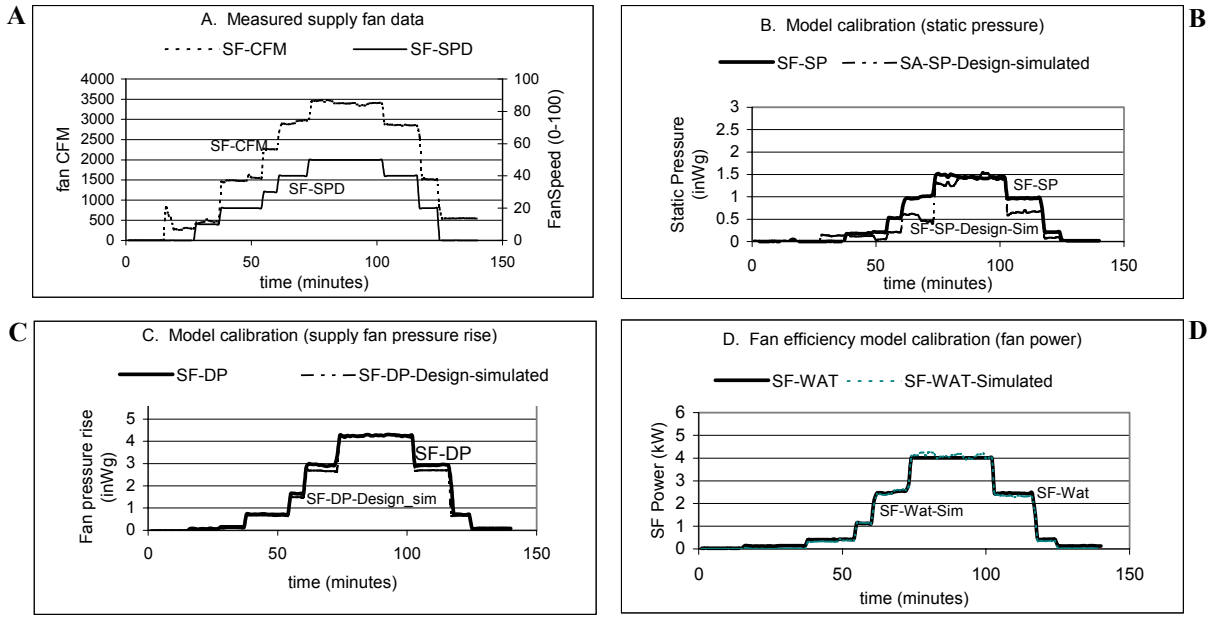

Figure 5. Supply fan calibration (experimental data).

the fan speed data, very much better agreement was obtained between the predicted and measured values. **Figure 5D** shows a comparison of the measured and predicted fan power. The predicted power does not depend on the fan speed and so is unaffected by the fault referred to above. The good agreement indicates the correctness of the efficiency model and of the value of the efficiency obtained from the manufacturer's data.

Modeling Using Measured Data From A Real Building

After the initial testing of the models using data from an experimental facility, the models were used in a field study to demonstrate their ability to simulate real systems.

Description Of The Building And Performance Data

The building in which the tests were performed is a 100,000 ft^2 commercial office building located in downtown San Francisco. The building has two chillers and one main air-handling unit. The AHU consists of a mixing box, a cooling coil, a supply fan and a return fan. The return fan is controlled so as to maintain a fixed pressure in the building. There is no heating coil in the air-handling unit and the heating load is satisfied by reheat coils in the terminal boxes in the exterior zones of each floor. Approximately half of the floors of the building are equipped with constant flow terminal boxes and the other half are equipped with variable-air-volume terminal boxes.

This building was built in 1960's and relatively little information regarding the mechanical system is available. The number and location of sensors is more representative of what is usually found in HVAC systems in commercial buildings. The supply and return airflow rates are not measured, neither is there a measurement of coil water leaving temperature or flow rate.

Functional Tests

Functional tests were performed on the mixing box and the supply fan. The tests were designed to be performed while the building was occupied, which required the tests to be relatively short and have limited impact on indoor thermal comfort. For each sub-system, both open loop and closed loop tests were performed. In the closed-loop tests, a number of different operating points were achieved by changing the controller set-point. Open-loop functional testing was conducted by overriding the controller and forcing the output to the desired positions. To determine the hysteresis of the actuators, step tests in both directions were scheduled for the mixing box dampers.

Calibration Procedure

The results of the functional tests were used to calibrate the models, following the procedures described above. Some changes in procedure were required because certain measurements or information that were available at the experimental facility were not available at the field test site:

No Airflow Data. As is often the case in commercial buildings, there was no measurement of supply or return airflow. Without an estimate of the airflow, it is not possible to predict the performance of fan and coils. However, in this building, the pressure rise and power were measured for both fans, so the airflow rates were estimated using equation (5).

No Fan Catalog Data. The lack of manufacturer's performance data precluded testing the fan based on design data. Since this is a common problem, an alternative approach that could be developed would be to use generic values for the initial values of the two constants, estimated based on diameter and fan type, and then fine tuned using functional test data.

Functional Tests And Modeling Results

Mixing Box. The results of the functional tests and modeling of the mixing box are shown in **Figure 6**. In order to avoid measurement errors due to incomplete mixing, the measured supply air temperature, corrected for the rise across the fan, is used as a proxy for the mixed temperature. An earlier set of tests had discovered significant leakage in both the return air dampers and outside air dampers. The measurements shown here were made after the building operator had fixed an actuator and improved the sealing of the dampers as much as he could. **Figure 6A** shows the test signal. **Figure 6B** shows the measured outside, return and mixed temperatures, together with the mixed air temperature predicted by a model that includes hysteresis. **Figure 6C** presents the outside air fraction, inferred from the temperature measurements, and the control signal. **Figure 6D** shows the estimated upper and lower limits of mixed air temperature using a 3:1 gain variation and assuming the acceptable leakage for each damper is 5%. The measured mixed air temperature is outside the permitted range at each end of the operating

range. In spite of the efforts of the building operator, the leakage was still ~11% when set for maximum outside air and ~28% for maximum return air. Such leakage levels result in significant increases in heating and cooling energy.

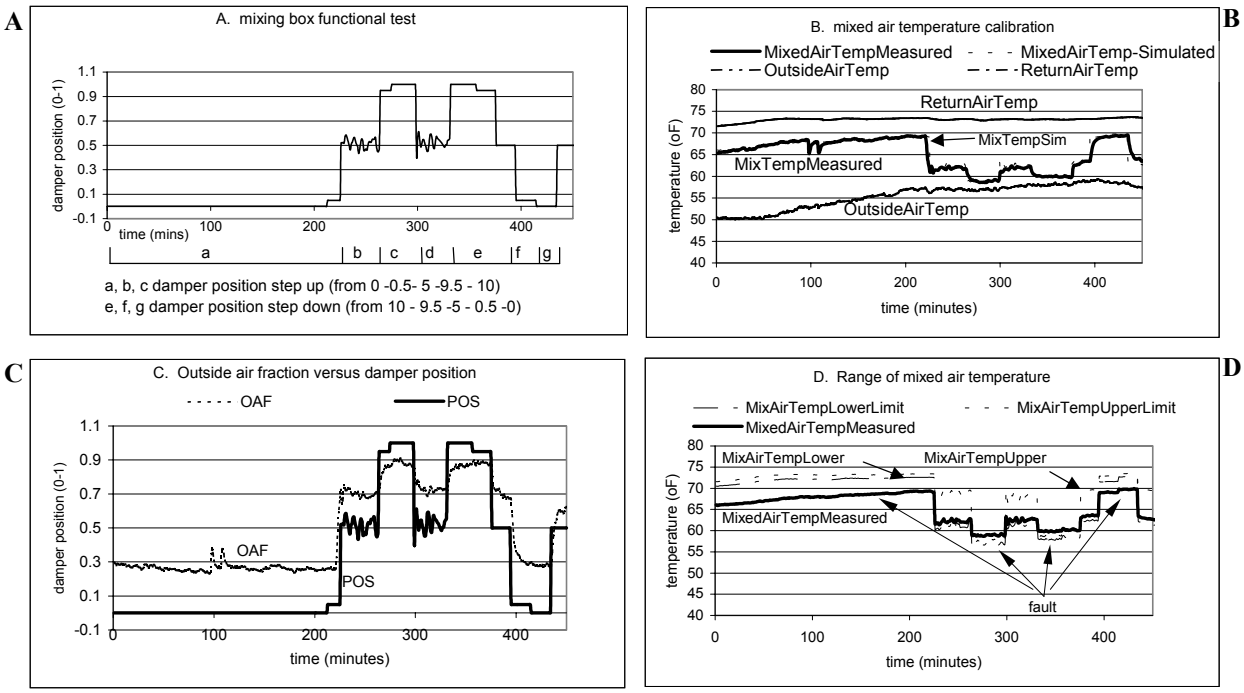

Figure 6. Mixing box test (field data).

Supply And Return Fans. **Figure 7** shows the test results for the supply and return fans. Because the building was occupied at the time, the tests cover only a limited part of the operating range.

Figure 7SA shows the different phases of the supply fan test. **Figure 7SB** is the comparison of the measured pressure rise across the fan and the pressure rise predicted by a model calibrated to fit the data. **Figure 7SC** is the comparison of the simulated and measured static pressure in the supply duct. There are greater fluctuations in the simulated pressure than in the measured pressure and the major cause is fluctuations in the fan speed. After talking with the building operator, it emerged that the supply fan has a problem with slipping belts, which leads to oscillation of the supply fan speed and power. This is corroborated by the estimated parameter values of the fan model; the efficiency of the supply fan is 5% lower than that of return fan, even though both fans are similar models from the same manufacturer and are the same age.

Figure 7RA-C shows the corresponding results for the return fan. The model generally agrees well with measured data for pressure rise and power rate. The fractional differences the between measured and simulated zone pressure is quite large but the absolute differences are relatively small compared to the fan pressure rise. Over the limited range of operation that could be covered in the tests, the model is able to achieve a good fit to the measured data for both the supply and return fans. This should allow the detection of faults such as increased resistance due to fouling of coils or filters or a change in the fan pressure rise *vs.* speed relationship due to incorrect wiring of the fan motor following electrical repairs. Changes in the efficiency of the fan and motor cannot be detected in the absence of a measurement of airflow rate.

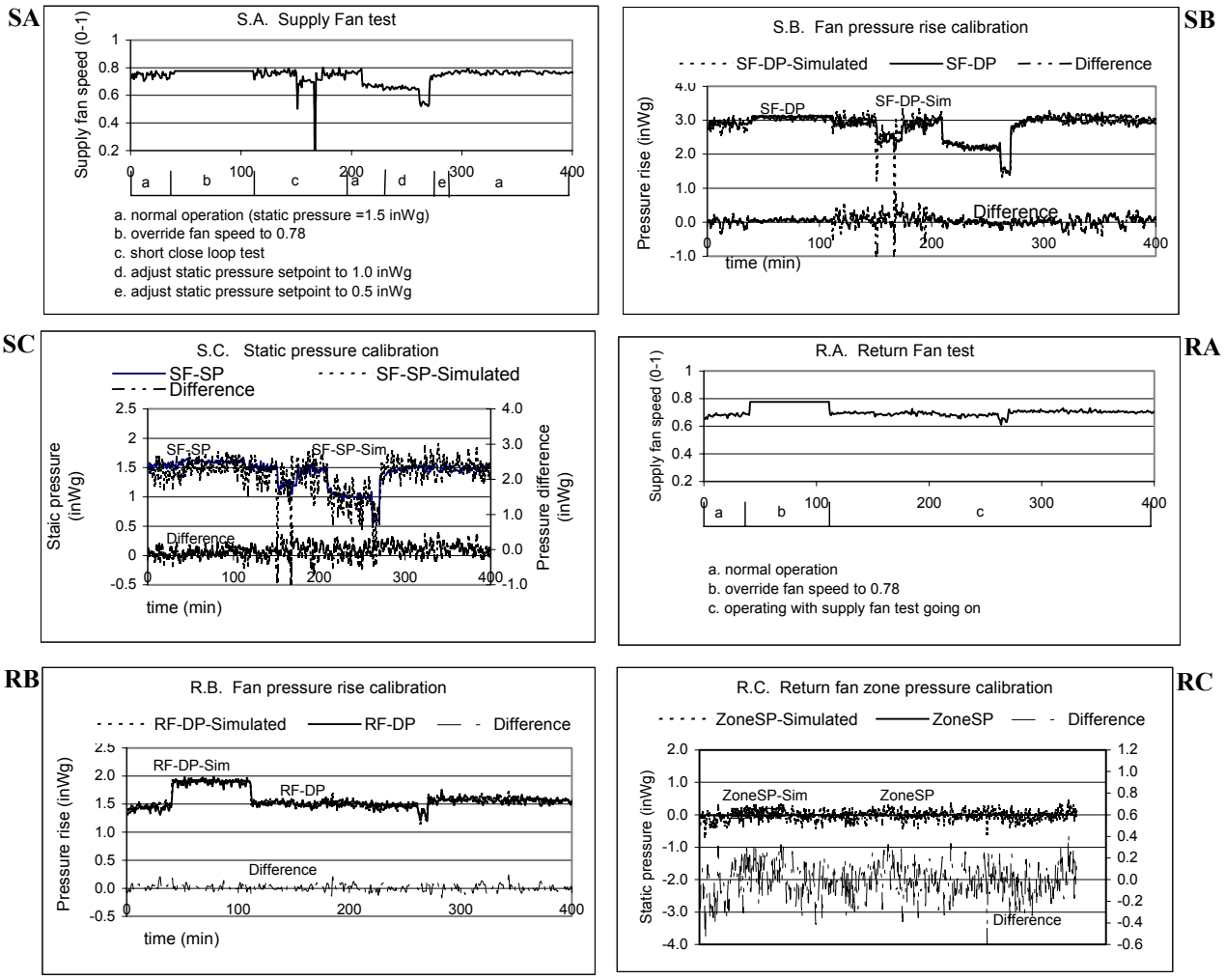

Figure 7. Supply and return fan test (field data).

Conclusions

The major objective of this study was to verify and demonstrate the use of HVAC equipment models for automated fault detection. Results from both an experimental facility and a commercial office building indicate that, once calibrated, the models tested could simulate the behavior of the mixing boxes and fan systems quite accurately. When calibrated using design information and manufacturers' data, the models were able to indicate the presence of a control signal offset fault in a variable speed drive. Leakage in a mixing box was successfully detected using a default model of acceptable operation. This indicates that such models are suitable for use in automated fault detection systems for functional testing and performance monitoring.

The next steps in the process of developing a model-based automated fault detection tool are to implement and test routines for determining when the differences between predicted and measured performance are significant, and hence indicate the presence of a fault. Since the models treat only steady state behavior, a routine to identify and disregard transient operation needs to be incorporated. A method of identifying and representing modeling and measurement errors across the operating range is also required in order to minimize false alarms while maximizing the sensitivity of the fault detection process. The resulting tool will then be field tested by connecting it on-line to an EMCS and using it both for functional testing and for monitoring of routine operation.

Acknowledgements

The authors wish to thank Johnson Controls Inc for providing measurements made at the Iowa Energy Center. They also gratefully acknowledge the assistance of John House, Dick Kelso, Tim Salsbury, Fred Smothers and Ted Ludwick. This work was supported by the California Energy Commission and by the Assistant Secretary for Energy Efficiency and Renewable Energy, Office of Building Research and Standards of the U.S. Department of Energy under Contract No. DE-AC03-76SF00098.

References

Brandemuehl, M. J., S. Gabel and I. Andersen. 1993. *A toolkit for secondary HVAC system energy calculations, HVAC2 Toolkit.* Prepared for The American Society of Heating, Refrigerating and Air Conditioning Engineers. TC 4.7 Energy Calculations. Atlanta, GA.: ASHRAE.

Benouarets, M., Dexter, A.L., Fargus, R.S., Haves, P., Salsbury, T.I., and Wright, J.A. 1994. *Model-Based Approaches to Fault Detection and Diagnosis in Air-Conditioning System, Proc. System Simulation in Buildings '94*, Liège, December.

McIntosh I.B.D, Mitchell J.W, Beckman W.A. 2002. *Fault detection and diagnosis in chillers - Part I: Model development and application.* ASHRAE Trans., Vol.106, Part 2, Paper number 4395, 268-282.

Ahn B.C, Mitchell J.W, McIntosh I.B.D. 2001. *Model-based fault detection and diagnosis for cooling towers.* ASHRAE Trans., vol.107, part 1, paper number AT-01-14-1, 839-846,

Haves, P. and Khalsa, S.K. 2000. "Model-based Performance Monitoring: Review of Diagnostic Methods and Chiller Case Study." *Proc. ACEEE Summer Study*, Asilomar, CA, August. LBNL-45949

Hyvarinen, J. 1997. IEA Annex 25 Final Report. VTT, Espoo, Finland.

LBNL. 1999. Proceedings of Diagnostics for Commercial Buildings: From Research to Practice, San Francisco, CA. http://poet.lbl.gov/diagworkshop/proceedings

Xu, Peng and Philip Haves. 2001. *Library of component reference models for fault detection (AHU and chiller).* Report to California Energy Commission. Berkeley, CA.: Lawrence Berkeley National Laboratory.

SPARK. 2002. *Simulation Problem Analyses and Research Kernel.* Lawrence Berkeley National Laboratory and Ayres Sowell Associates, Inc. Berkeley, CA.:
Lawrence Berkeley National Laboratory. http://gundog.lbl.gov